



**S-N CHARACTERISTICS OF
NOTCHED SPECIMENS**

by
Clarence R. Smith

Prepared For

NATIONAL AERONAUTICS AND SPACE ADMINISTRATION

CONTRACT NAS 3-7268

GENERAL DYNAMICS
Convair Division

FINAL REPORT

S-N CHARACTERISTICS OF NOTCHED SPECIMENS

by

Clarence R. Smith

prepared for

NATIONAL AERONAUTICS AND SPACE ADMINISTRATION

June 15, 1966

CONTRACT NAS3-7268

Technical Management
NASA Lewis Research Center
Cleveland, Ohio
Materials and Structures Division
Marvin H. Hirschberg

GENERAL DYNAMICS

Convair Division

ABSTRACT

24081

Fatigue test data and analyses are presented indicating that the results of a single fatigue test in the short life range plus mechanical properties of the material are all that is needed to predict S-N characteristics of notched specimens for tension-tension loading. Independent of nominal stress or stress concentration, the method is applicable to structural parts where neither average stresses nor stress concentrations are known.

While confirmed by tests on 7075-T6 aluminum alloy only, the method should be applicable to most alloys having a low sensitivity to strain hardening or softening.

Author

TABLE OF CONTENTS

SECTION		PAGE
1	INTRODUCTION	1
2	TEST PROGRAM	3
	MATERIAL	3
	SPECIMENS	3
	FIXTURES	3
	TESTING MACHINES	3
	TEST RESULTS	6
3	THEORY AND COMPARISON OF PREDICTED AND TEST LIVES	11
	SMITH METHOD	11
	NASA LEWIS METHOD	15
	MODIFIED NASA LEWIS METHOD	17
4	DISCUSSION	24
5	CONCLUSIONS	25
6	REFERENCES	26

LIST OF TABLES

TABLE		PAGE
I	Mechanical Properties of 0.050-inch Thick 7075-T6 Aluminum Alloy	27
II	Constant-Amplitude Data for Unnotched 0.050-inch 7075-T6 Aluminum Alloy	28
III	Constant-Amplitude Data for Notched ($K_t = 2.6$) 7075-T6 Aluminum Alloy -- $R = 0$	30

LIST OF ILLUSTRATIONS

FIGURE		PAGE
1	Specimens for Fatigue Program	4
2	Lateral Support Fixture for Compressive Fatigue Loading	5
3	Stress-Strain Curve for 7075-T6 Aluminum Alloy	7
4	S-N Curves for Axially-loaded Unnotched Specimens of 7075-T6 Aluminum Alloy	8
5	Maximum Stress versus Cycles to First Crack or Failure for Notched 7075-T6 -- R = 0	9
6	Maximum Stress versus Cycles to First Crack or Failure for Notched 7075-T6 -- R = -1	10
7	S-N Curves for 7075-T6 showing Maximum Stress Cutoff for Stress at Concentration	12
8	Comparison of Test and Predicted Lives to First Crack by Smith Method	13
9	Comparison of Test and Predicted Lives to Failure by Smith Method	14
10	Comparison of Test and Predicted Fatigue Lives to Failure by Equation (1) and Reference Datum Points	16
11	Constant Life Curves for 7075-T6 Aluminum Alloy	18
12	Relation between Strain Cycling at R = -1 and R = 0	19
13	Effect of Cyclic Loading on Stress-Strain Curve of 7075-T6 Aluminum Alloy	20
14	Comparison of Test and Predicted Lives to First Crack by Modified NASA Lewis Method	22
15	Comparison of Test and Predicted Lives to Failure by Modified NASA Lewis Method	23

1 INTRODUCTION

This research program was sponsored by NASA Lewis Research Center under Contract NAS3-7268. The overall objective of this investigation is to obtain a method whereby S-N characteristics of notched specimens can be predicted, given static tensile properties for the material and a datum point representing the fatigue life of such specimens for a given loading. The present program is limited to 7075-T6 aluminum alloy, tests on notched and unnotched specimens being included as part of the investigation.

A method for using static tensile properties of a material for relating strain range to fatigue life was developed by NASA Lewis Research Center^{1, 2} which can be expressed by the following equation:

$$\Delta \epsilon = \frac{3.5 \sigma_u}{E N_f^{0.12}} + \frac{D^{0.6}}{N_f^{0.6}} \dots \dots (1)$$

where

σ_u = ultimate tensile strength, psi

D = ductility, $\ln \frac{100}{100 - RA}$

RA = reduction in area, percent

N_f = number of cycles to failure

The validity of the method has been amply confirmed by test data for many alloys (Ref. 1, 2). Being valid for reversed straining ($R = -1$) only, the method in its present form is not applicable to many structural components subjected to unidirectional loading or where tensile and compressive loading are of unequal magnitude.

The Smith method^{3, 4} of predicting fatigue life is based on the use of a single datum point representing the life of a structure (or notched specimen) in the short life range to estimate the stress range at point of crack initiation. The stress range is then prorated directly for other loads to establish S-N characteristics of the structure. Of special importance is the fact that neither nominal stress nor stress concentration are needed; however, a family of S-N curves and a stress-strain curve for the material are required.

It was first thought that by using some form of Goodman diagram to translate strain ranges for reversed loading (as obtained from Equation 1) in terms of S-N curves for unnotched material the Smith method could then be used for predicting S-N characteristics of notched specimens. As it turned out, a form of Goodman diagram was used to provide information instrumental in modifying Equation (1) for cycling at other than $R = -1$. This permits using the basic premise of the Smith method (that of using a single datum point) to estimate lives of notched specimens for various fatigue loadings, using strain ranges obtained directly from mechanical properties of the material. Hereinafter noted as the Modified NASA Lewis method, it overcomes one of the basic faults of the Smith method in that S-N properties of unnotched material are not required.

While the present program is limited to 7075-T6 aluminum alloy, applicability to other materials is highly probable in view of the preponderous data support for many materials of the basic NASA Lewis method (Ref. 1, 2).

2 TEST PROGRAM

MATERIAL

The material for the specimens used in this program was nominally 0.050 in. thick 7075-T6 aluminum alloy. Yield strength varied between 74,500 psi and 79,600 psi for an average of 76,000 psi. Ultimate strength varied between 82,900 psi and 86,700 psi for an average of 84,000 psi. Average elongation and reduction in area were 11.1 percent and 26.4 percent, respectively. Mechanical properties are shown in Table I.

SPECIMENS

Notched and unnotched specimens were made according to the sketches shown in Figure 1. The end holes shown were not used for reacting the cyclic load. Being located along the centroidal loading axis, their purpose was for aligning the specimen in the end clamping fixtures prior to clamping. In all cases, special care was exercised in finishing the edges of the unnotched specimens, using a 150-grit emery paper paper. All polishing operations were in the direction of the specimen longitudinal axis. Previous experiments have shown that finishing in this manner provides the same fatigue life as that obtained for specimens having a final buffing. Tensile tests were made using MIL-151 specimens.

FIXTURES

Two fixtures were used for providing lateral support during compressive loading-- one for unnotched specimens and the other for notched specimens. The fixture for notched specimens had a 3/8 in. diameter hole near the center to permit visual inspection for cracks during test; otherwise, both fixtures were the same. An 0.0015 clearance along the test section was provided by shimming the grip ends prior to tightening, using an 0.0015 feeler gage to check clearance after securing. As previously discussed, aligning was achieved by preloading the specimen through the end holes and tightening the end grips while the preload was maintained. A schematic of the support fixtures is shown in Figure 2.

TESTING MACHINES

Tensile Tests

Tensile tests were made in a Tinius-Olsen mechanical driven universal testing, using a strain rate of 0.005 inch per inch per minute.

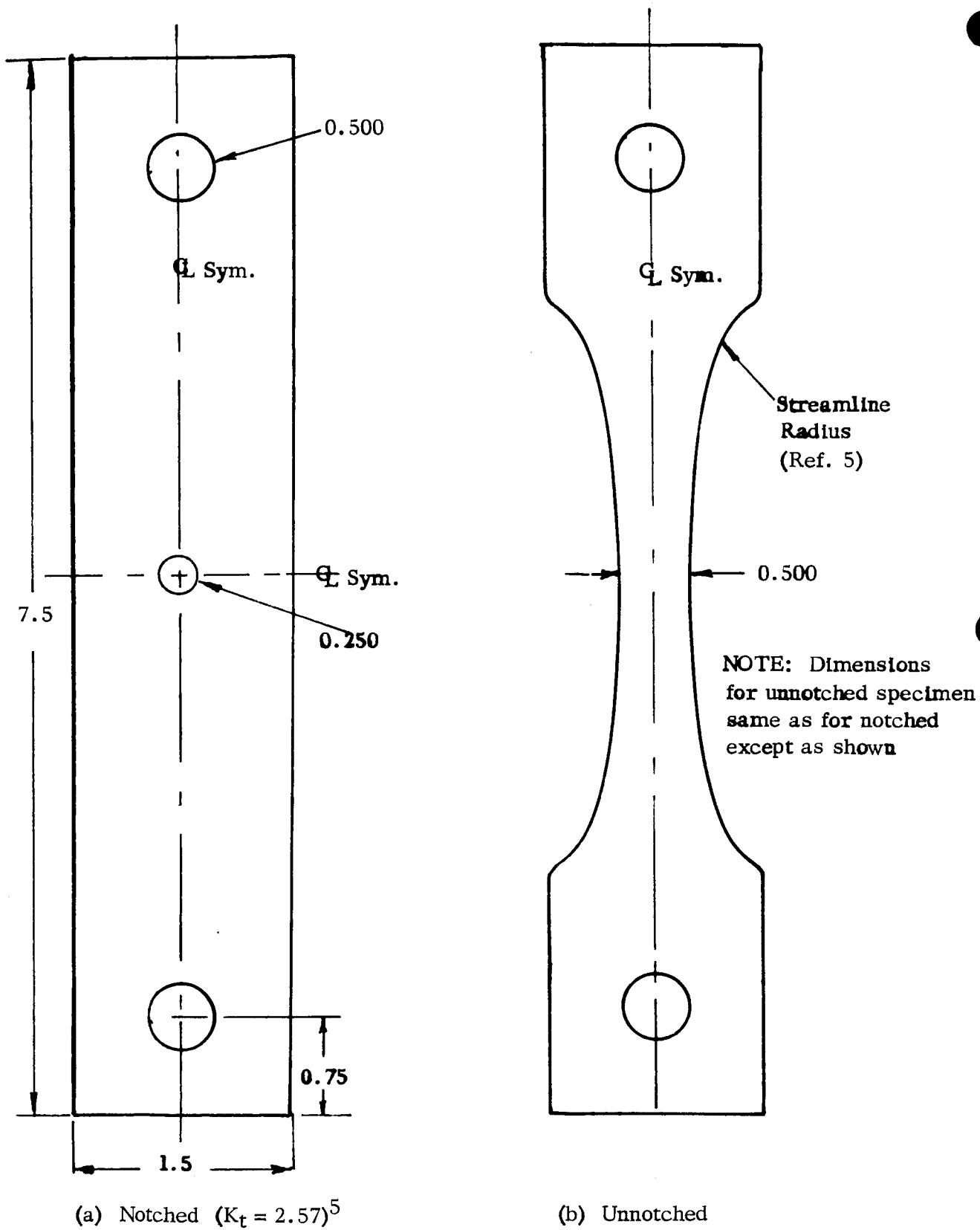


Figure 1. Specimens for Fatigue Program

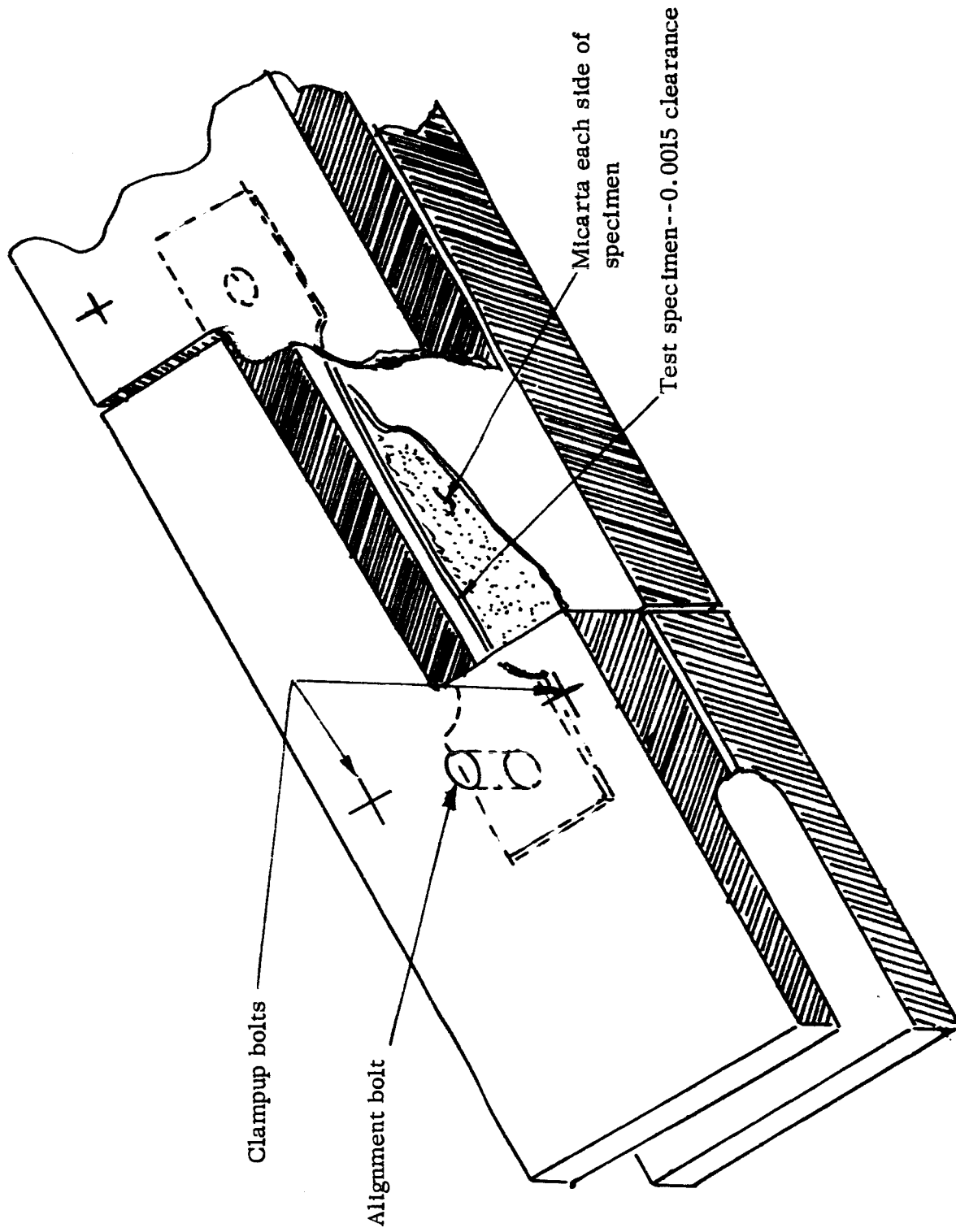


Figure 2. Lateral Support Fixture for Compressive Fatigue Loading

Fatigue Tests

Fatigue tests for lives in excess of 10,000 cycles were usually made in a Sonntag constant-load type fatigue testing machine. For lives of below 10,000 cycles (in some cases above) a Tatnall-Budd hydraulically operated fatigue testing machine was used. Rate of loading for the Sonntag machine was 1750 cpm, while 5 cps was used for the Tatnall-Budd machine. All fatigue testing machines were calibrated at 6 month intervals.

Cracks in notched specimens were detected visually, using a low power magnifying glass as an aid. The procedure was to test one specimen to failure without crack observations and subsequently make observations at from 6 to 10 percent increments of the failing life, starting at fifty percent of failing life.

Several aids were used, including die-check, crack wires; however, cracks which were detected in this manner were also visible to the naked eye. Investigation with eddy-current showed promise; however, this required removal of the lateral support fixture and was considered more work than it was worth. Comparative tests with die-check showed no effect on fatigue life; however, the use of die-check was discontinued because it was no more effective than inspection with magnifying glass.

TEST RESULTS

Tensile Tests

Results of tensile tests are presented in Table I and a stress-strain curve for 7075-T6 aluminum alloy is given in Figure 3. Average properties are as follow:

Ultimate strength . . .	84,000 psi
Yield strength (0.2%) . . .	76,000 psi
Elongation	11.1 percent
Reduction in area	26.4 percent

Fatigue Tests

Data for unnotched specimens are presented in Table II and graphs of maximum stress versus cycles to failure are presented in Figure 4 for R = 0, -0.5 and -1. Data for notched specimens are presented in Table III and graphs of maximum stress versus cycles to first crack or failure are presented in Figures 5 and 6.

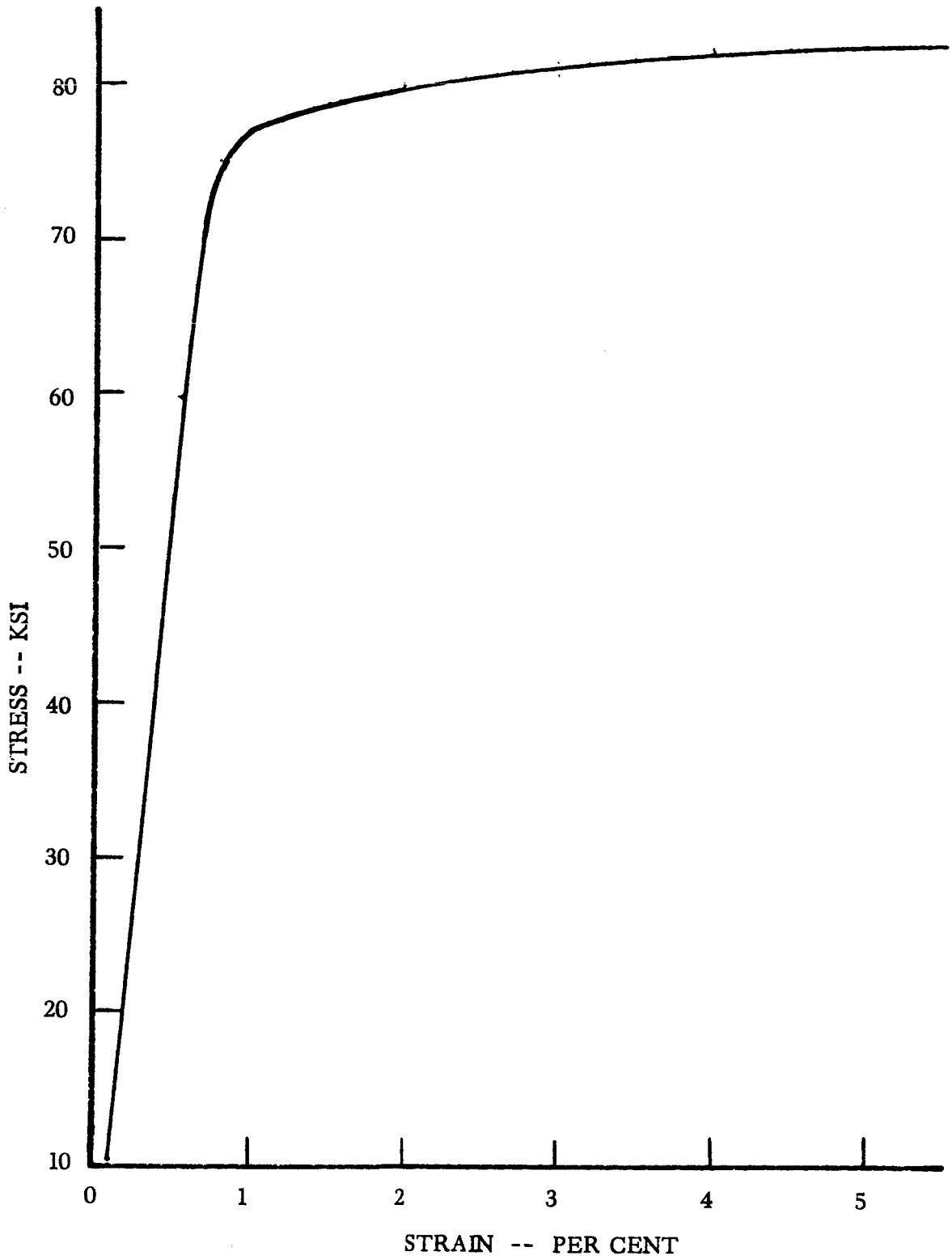


Figure 3. Stress-Strain Curve for 7075-T6 Aluminum Alloy

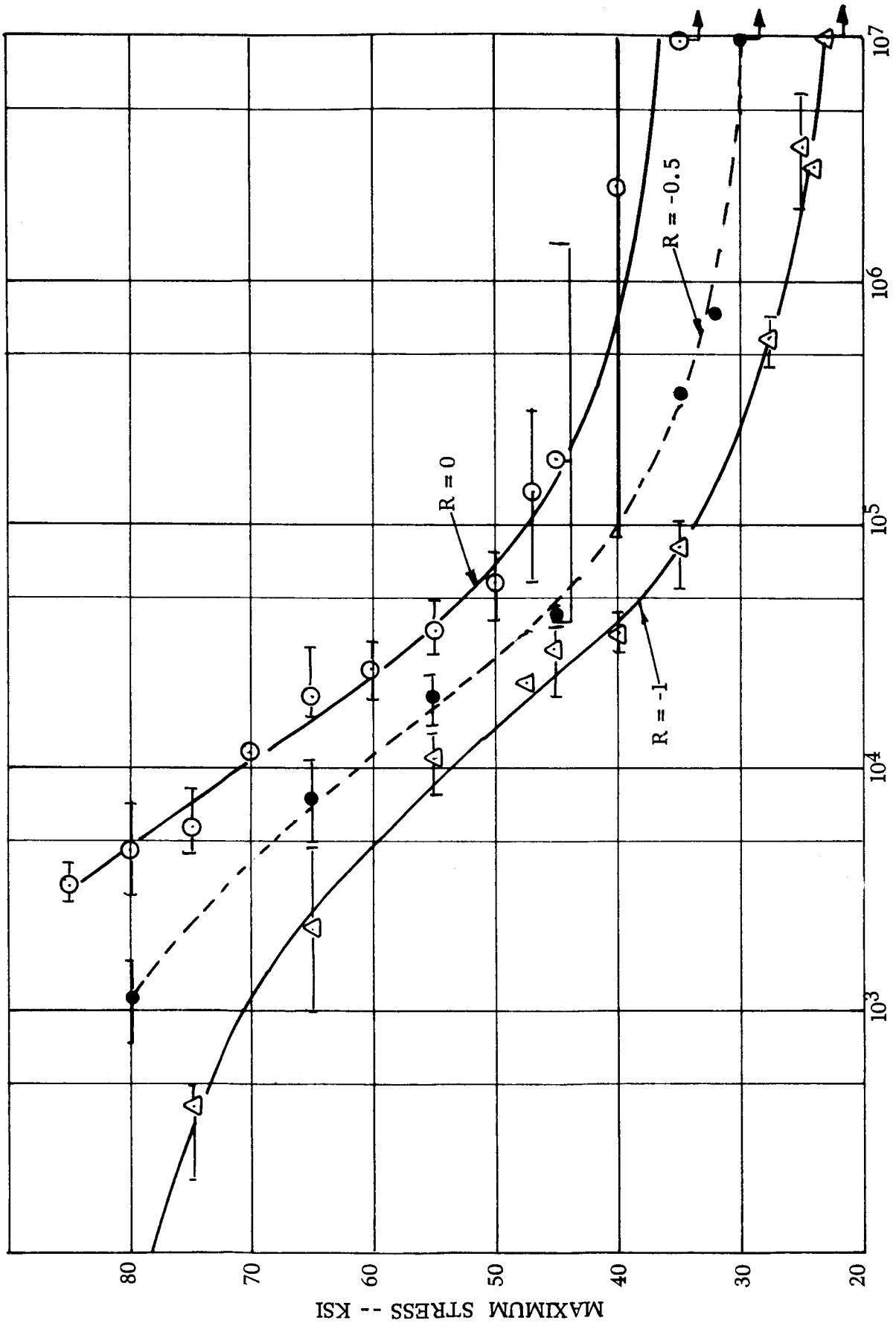


Figure 4. S-N Curves for Axially-loaded Unnotched Specimens of 7075-T6 Aluminum Alloy

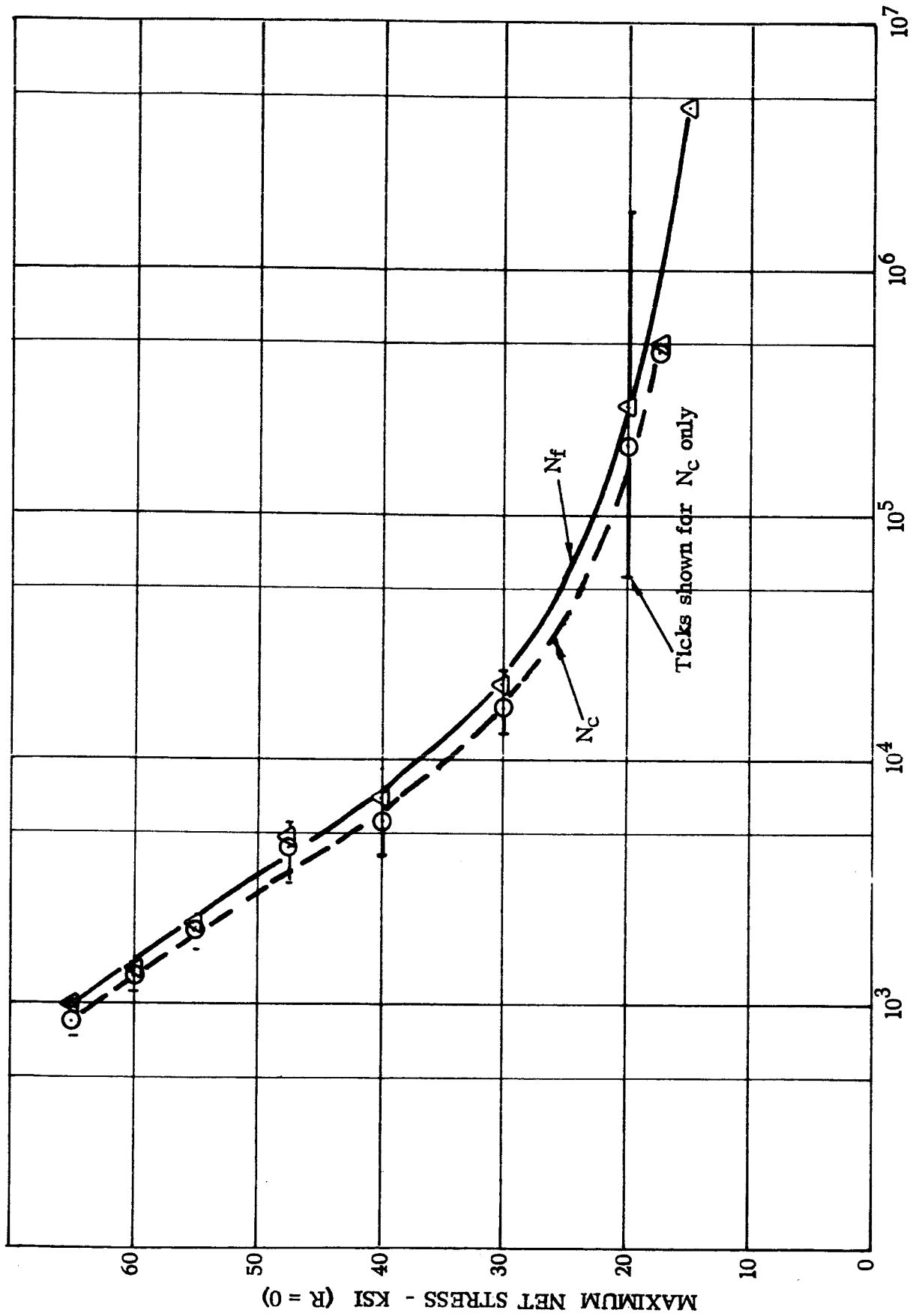
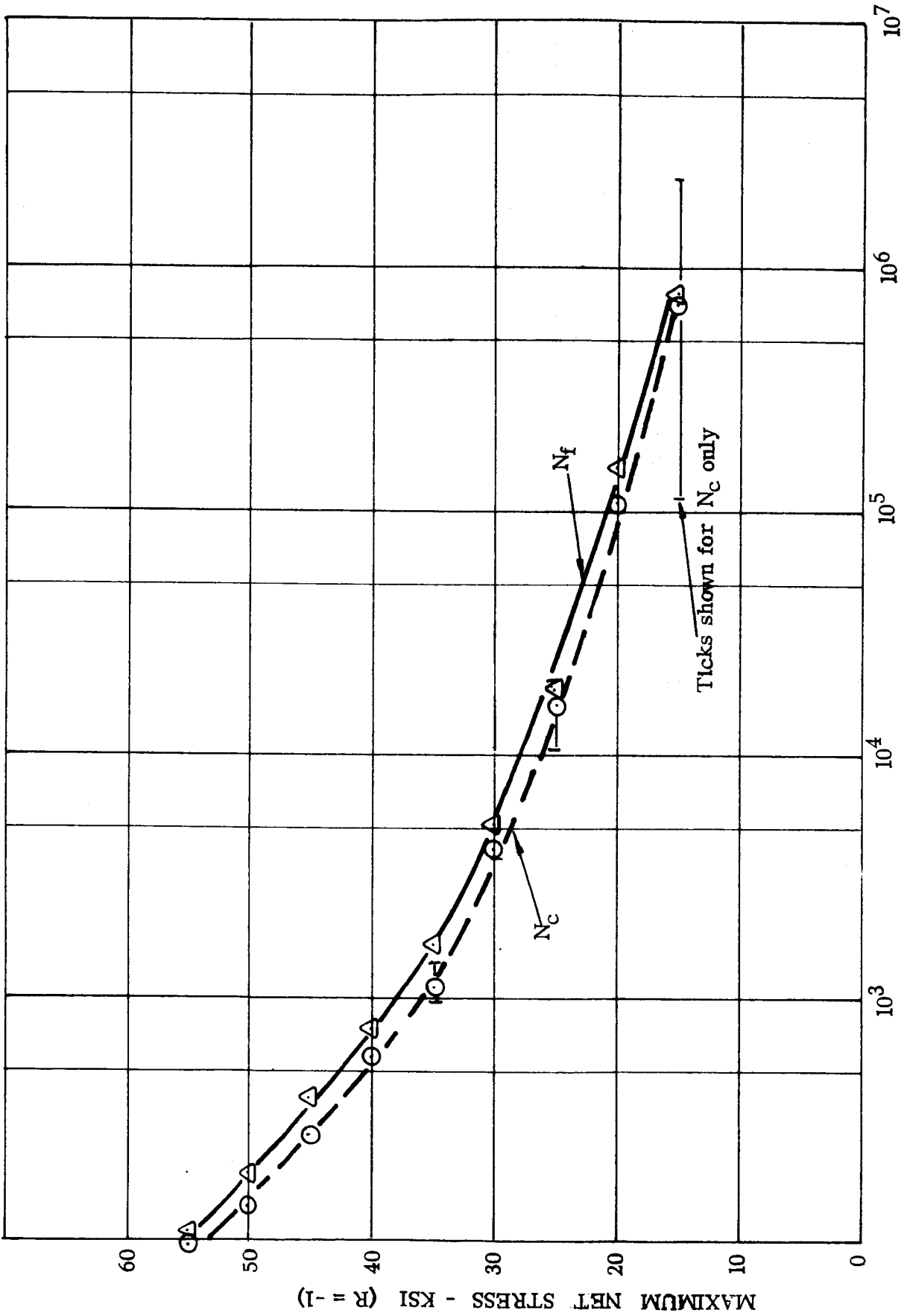


Figure 5. Maximum Stress versus Cycles to First Crack or Failure for Notched 7075-T6 ($K_t = 2.57$)



3. THEORY AND COMPARISON OF PREDICTED AND TEST LIVES

SMITH METHOD

The method of predicting fatigue life known as the Smith method (Ref. 3 and 4) is in reality not a method of predicting fatigue life at all. Rather, it is a method of using a constant-amplitude fatigue test of a part or structure to determine the stress range at the point of crack initiation. Knowing the stress range, it is then possible to use S-N data for unnotched specimens of the same material to predict life of the part for other loads, being careful to include effects of residual stresses while using the stress range to prorate stresses for other loads. Since loads can be prorated directly, there is no need to know nominal stress nor stress concentration. However, a family of S-N curves for unnotched material is needed.

The S-N curves of Figure 4 for unnotched specimens are replotted in Figure 7 with fractional stress ratios interpolated between $R = -1$ and $R = 0$ above the proportional limit. A line representing the maximum stress attainable at a concentration is also shown, the development of which is described in References 3 and 4. In essence, the cutoff represents the maximum stress attainable at the concentration by virtue of the local strain being limited by the strain away from the concentration still in the elastic range. Thus, a notched specimen cycled at a loading ratio of zero (ratio of minimum load divided by maximum load) that fails after 1250 cycles experiences a maximum stress of 76,800 psi and a minimum stress which is the stress ratio (R) at the cutoff times the maximum stress which in this case amounts to $-0.62 \times 76,800$ psi or -47,000 psi. The total stress range is the algebraic difference between maximum and minimum stress amounting to 124,400 psi. A shortcut is to perform the subtraction prior to multiplying, e.g. $1 - (-0.62) = 1.62$ which when multiplied by 76,800 psi equals 124,400 psi.

Similar manipulations will determine stress ranges for other lives within the cutoff range. In each case, the negative stress ratio indicates a residual compressive stress (although the permanent strain may be positive). The residual stress is limited by the compressive yield strength of the material which, after yielding in tension, is reduced by the Bauschinger effect. It is assumed that a stress ratio of -0.9 is the limiting value in Figure 7.

Having obtained the stress range for a given loading, it is a simple matter of prorating for other loads to find appropriate S-N values from the unnotched data in Figure 7. In cases where the prorated stress range is greater than the proportional limit for the material, it is necessary to obtain a maximum stress and stress ratio that agrees with the cutoff. For example, prorating the 124,400 psi stress range for loading at 80 percent of the referenced loading (the load that caused failure in 1250 cycles) indicates a stress range of 99,500 psi. This conforms with a maximum stress of 75,600 psi at a stress ratio of -0.32 for a life of 3200 cycles as found in Figure 7.

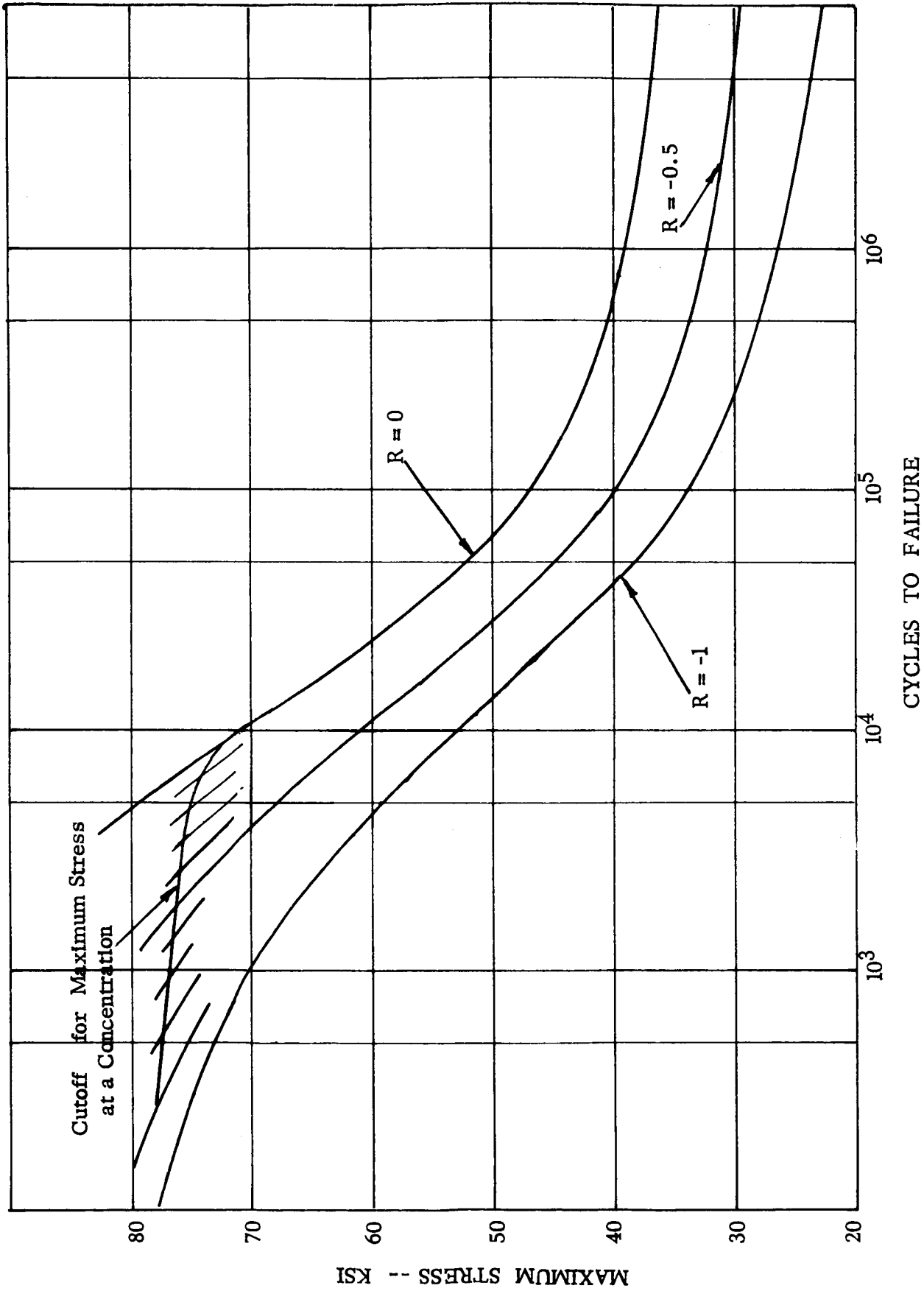
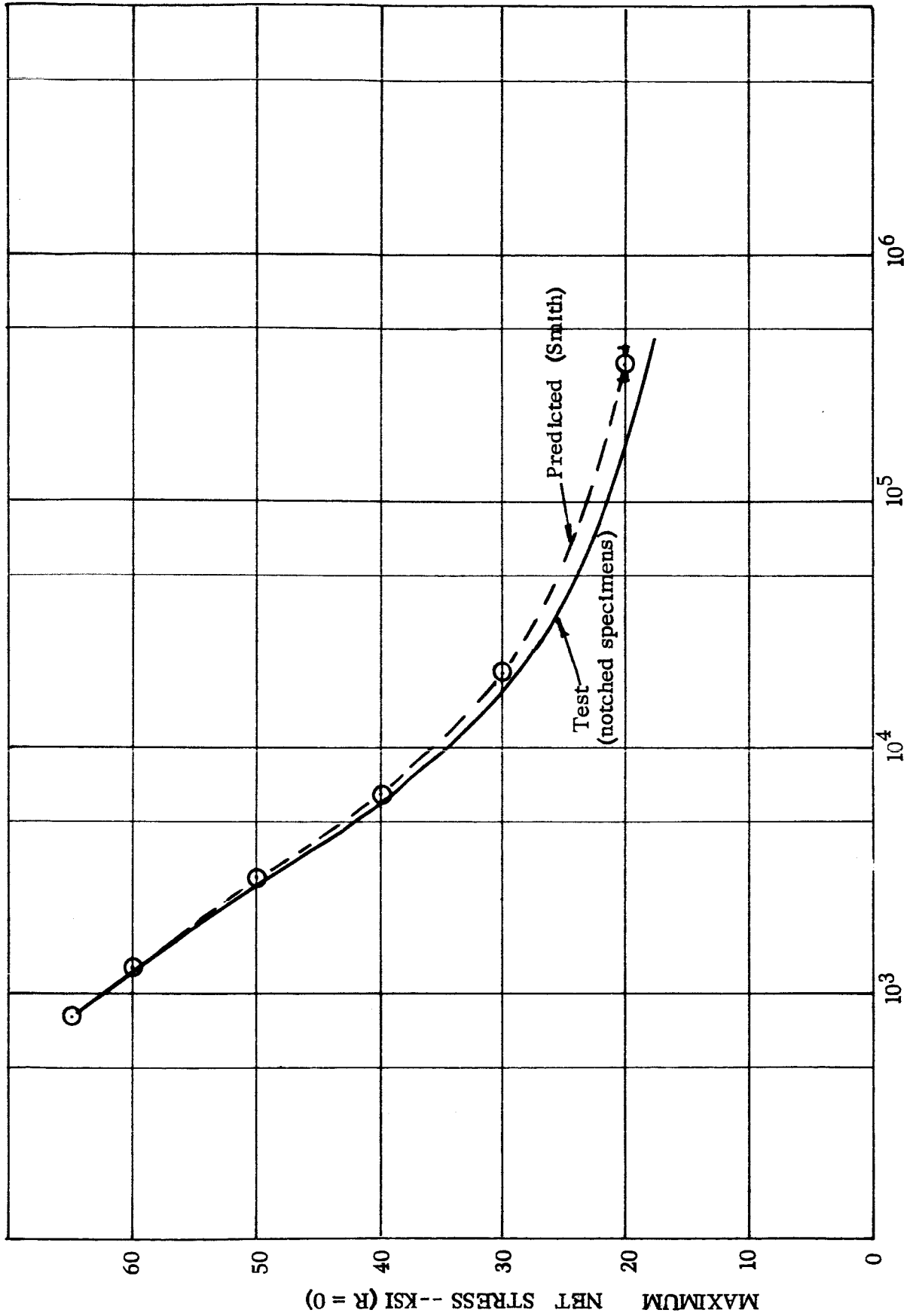
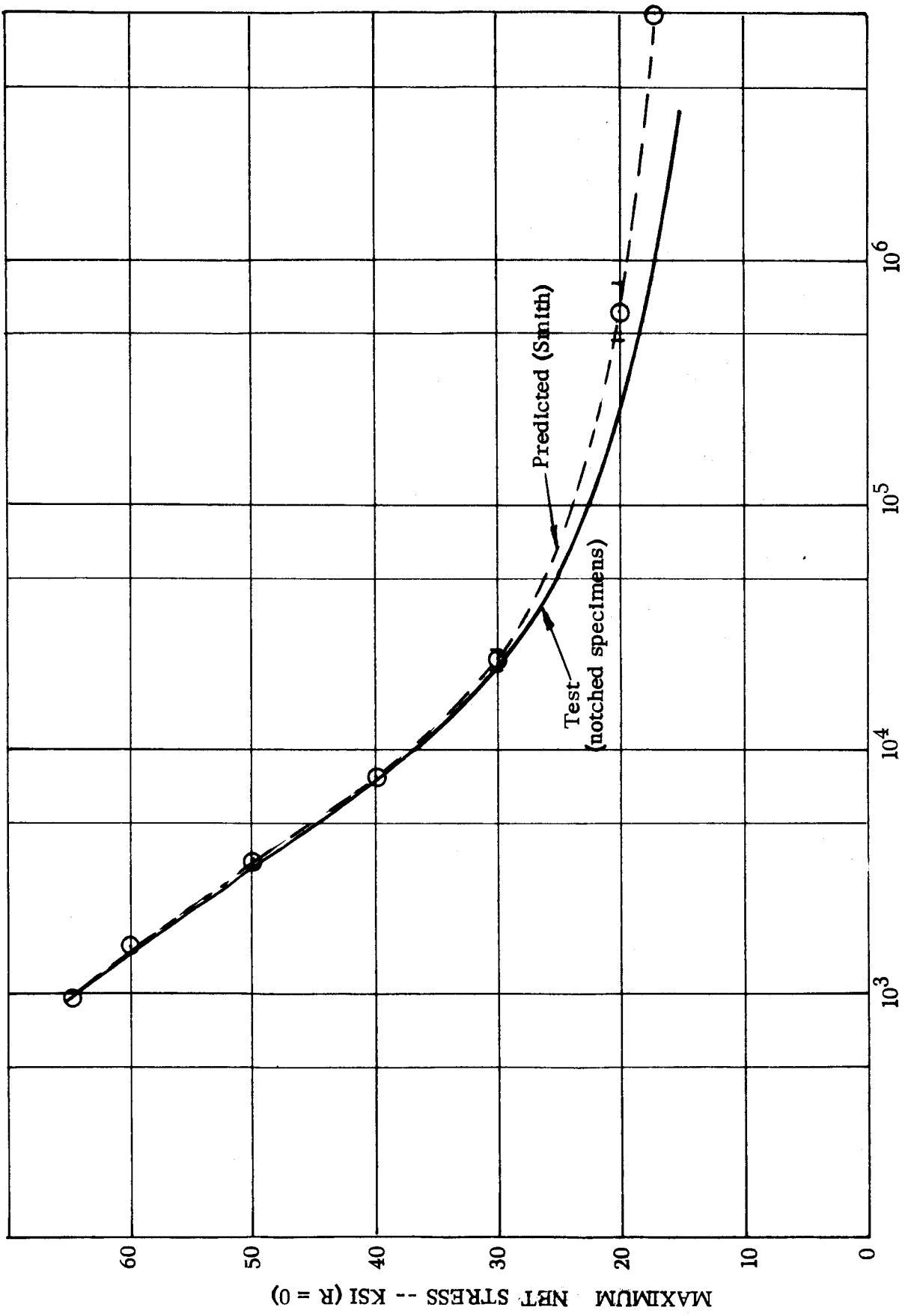


Figure 7. S-N Curves for 7075-T6 showing Maximum Stress Cutoff for Stress at Concentration

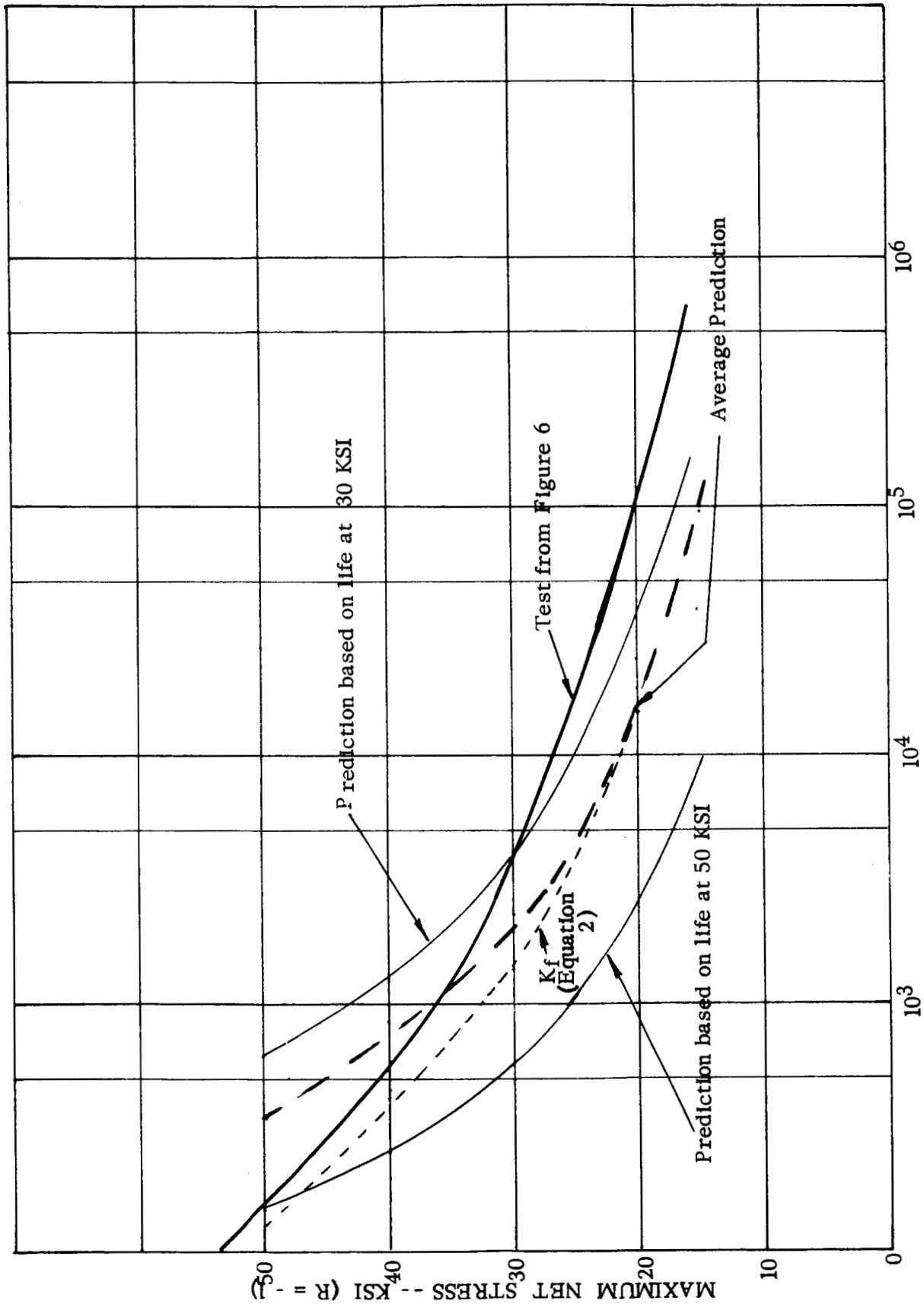


CYCLES TO FIRST CRACK

Figure 8. Comparison of Test and Predicted Fatigue Lives to First Crack by Smith Method



CYCLES TO FAILURE
 Figure 9. Comparison of Test and Predicted Fatigue Lives to Failure by Smith Method



CYCLES TO FIRST CRACK

Figure 10. Comparison of Test and Predicted Fatigue Lives to Failure by Equation (1) and Reference Datum Points

MODIFIED NASA LEWIS METHOD

Equation (1) relates fatigue life to strain range for reverse loading. It assumes a knowledge of the nominal strain and strain concentration. While providing excellent agreement with test data for many materials (Ref. 1, 2), Equation (1) is limited in that it applies to reverse loading only. Inasmuch as most aerospace components are subjected to various types of loading, of which reversed is but one, it would be desirable to obtain a relationship (or relationships) applicable to all types of loading. It would also be desirable to use a reference fatigue datum point (as in the Smith method). This would enable predicting S-N characteristics of a part given conventional tensile properties of the material and a single datum point representing the short life fatigue strength of the part. As in the Smith method, a life short enough to ensure some localized plastic strain is desirable to relieve fabrication stresses; e.g., fabrication stresses usually vary for identical parts.

According to a Goodman diagram, a relationship exists between lives for reversed loading and loading at other stress ratios, static tensile ultimate strength of the material being a parameter common to all ratios. While the Goodman diagram has been found wanting in many instances, a glance at the S-N curves in Figure 4 indicates that some kind of relation should exist between life, maximum stress, and stress ratio.

Data from Figure 4 are plotted in the form of constant-lifetime curves in Figure 11, using semi-log graph paper so that maximum stress is shown on the log scale and stress ratio on the linear scale. Note that the graphs are nearly parallel. Considering the stress range for $R = -1$ to be $2\sigma_{\max.}$, an average ratio of the stress range for $R = 0$ divided by the stress range for $R = -1$ turns out to be about 0.7. Assuming the strain ranges are proportional (at least between 5×10^4 and 10^7 cycles) to stress ranges, an expression for $R = 0$ can be had by simply multiplying the coefficients on the right of Equation (1) by 0.7 so that the following equation results:

$$\Delta\epsilon = \frac{2.45 \sigma_u}{E N_f^{0.12}} + \frac{0.70 D^{0.6}}{N_f^{0.6}} \dots \dots (3)$$

Relations for any other stress ratio can be found in a similar manner; however, the maximum stresses of Figure 11 must be multiplied by a factor representing the algebraic difference between maximum stress and minimum stress for the appropriate stress ratio. For $R = -0.5$ this factor would be $1 - (-0.5)$ or 1.5. Graphs for $R = 0$ and $R = -1$ are presented in Figure 12.

Equation (3) is inapplicable where much plastic deformation takes place since the strain cycle for $R = -1$ continues to increase while that for $R = 0$ is more or less limited by the elastic component of strain after the first cycle. This is shown in Figure 13 which is a reproduction of a load-strain diagram taken directly from the testing machine. Each broad line represents ten cycles after which load is raised and cycling repeated at the higher load.

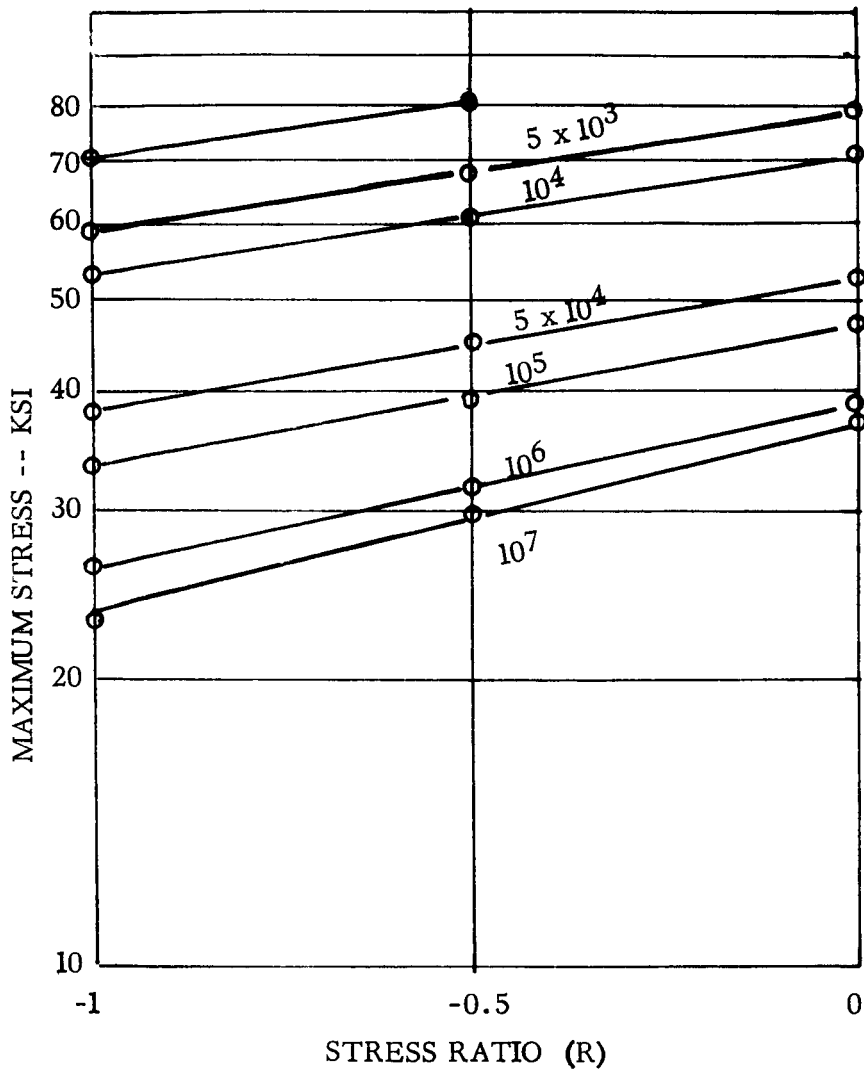
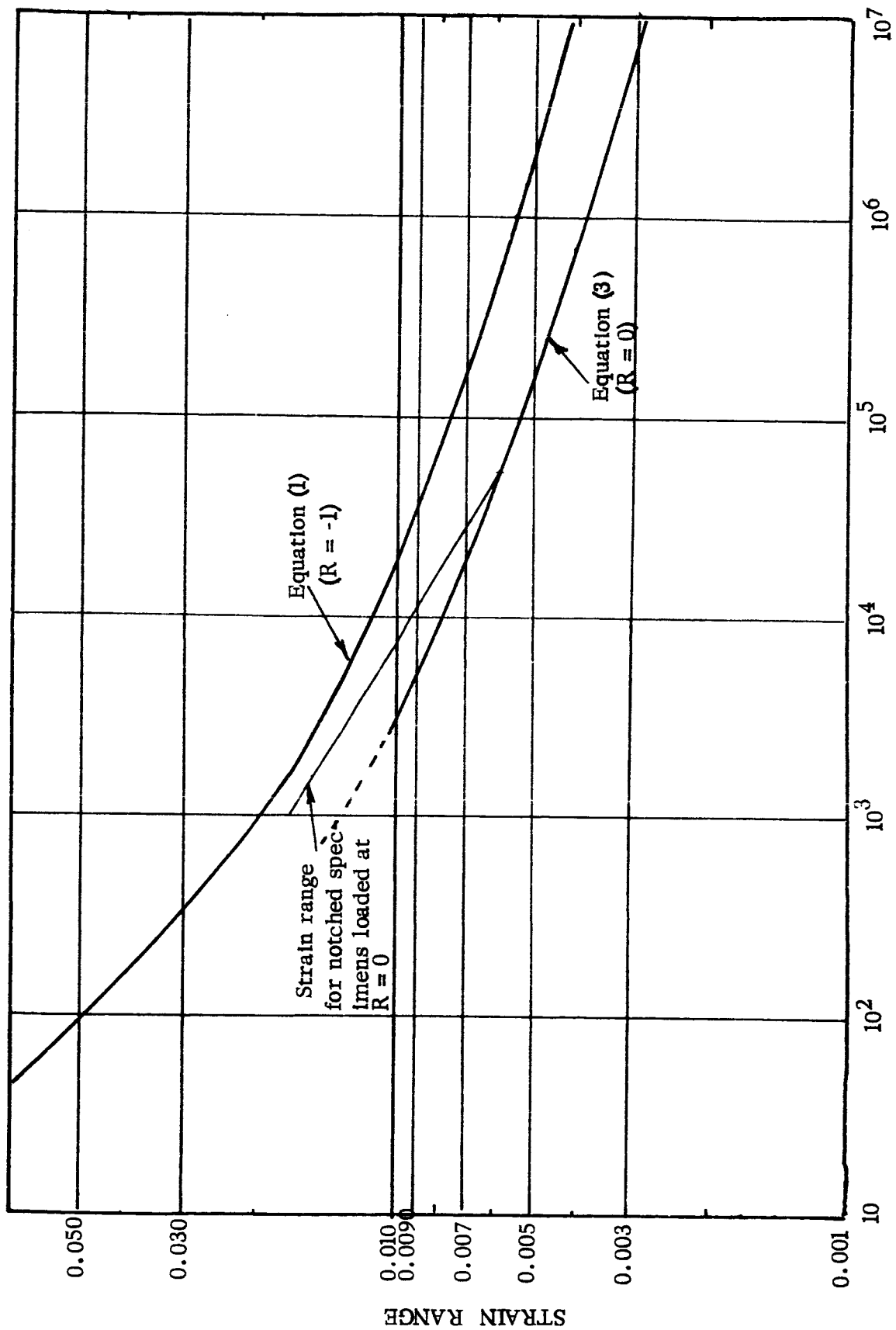


Figure 11. Constant Life Curves for 7075-T6 Aluminum Alloy



FATIGUE LIFE -- CYCLES

Figure 12. Relation between Strain Cycling at $R = -1$ and $R = 0$

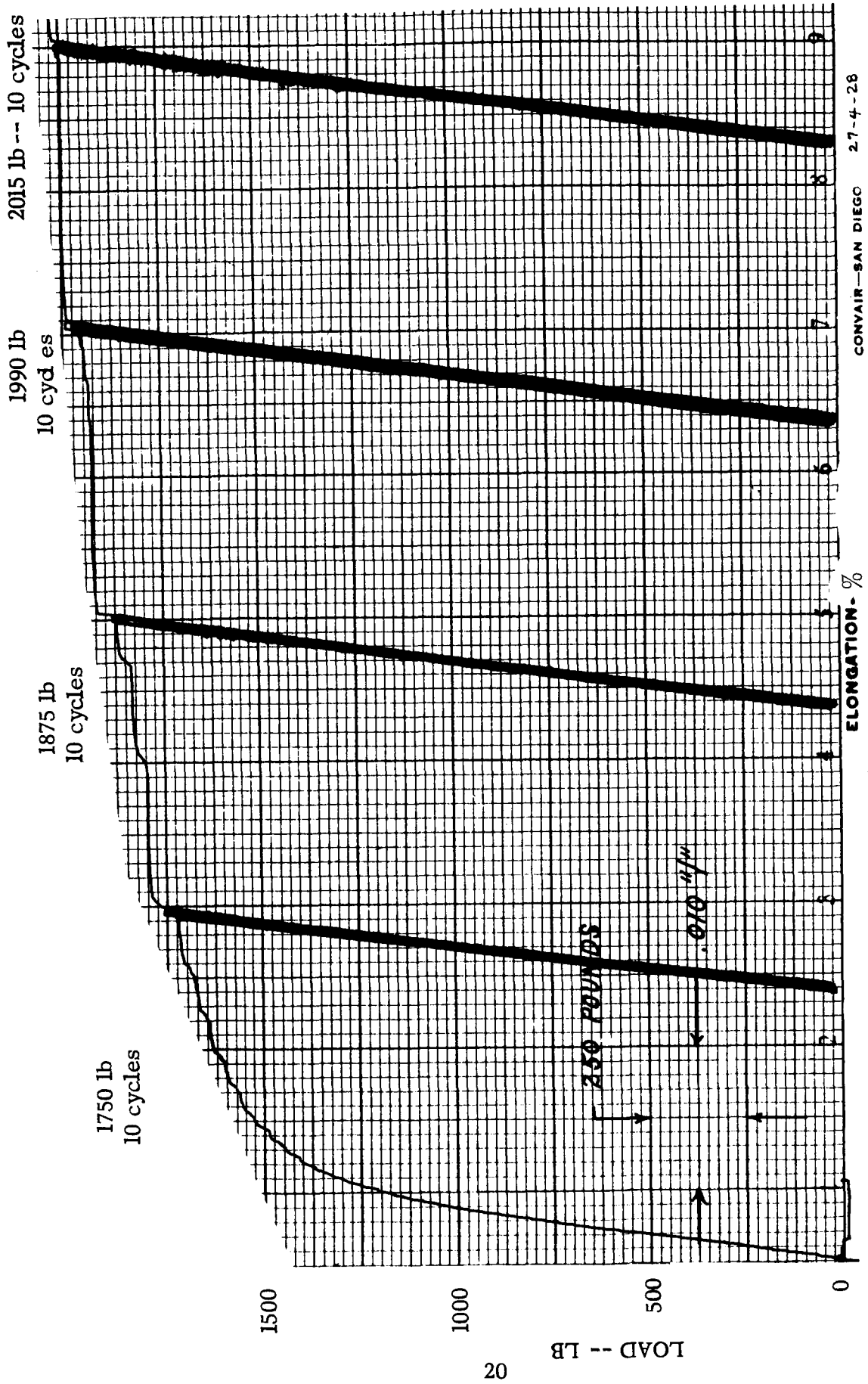


Figure 13. Effect of Cyclic Loading on Stress-Strain Curve of 7075-T6 Aluminum Alloy

While it would be possible to project the curve for $R = 0$ (Equation 1) to shorter lives by using empirical data in conjunction with Equation (1), such a manipulation would be of no value for predicting lives of notched specimens. As shown for the Smith method, the stress range (and presumably the strain range) takes on characteristics of partially reversed stressing when yielding occurs at the notch. Accordingly, strain ranges for lives of fewer than 10^4 cycles (say 5×10^4 cycles for good measure) should fall between the curves described by Equations (1) and (2).

With the object of finding a locus of strain ranges which would permit prorating loads for predicting fatigue life (as in the Smith method), a straight line starting at 1500 cycles and strain range of 0.015 (Ref. Fig. 12) which intercepted the curve for $R = 0$ (Equation 2) at 5×10^4 cycles provided excellent agreement with test data. Predictions are compared with test data in Figures 14 and 15. Here, Equation (2) was used to predict lives where prorated strain ranges fell below 0.006, the straight line for larger strain ranges. The black triangles represent average predictions based on reference strain ranges corresponding to 60, 50, and 40 KSI loading. Ticks for variations in predictions are not shown as the worst discrepancy was from 1.3×10^6 cycles, based on 60 KSI loading, to 1.5×10^6 cycles when estimates were based on the strain range at 40 KSI.

As an illustrative example, the life to first crack of notched specimens (average) is 1250 cycles when loaded at $R = 0$ to an average P/A stress of 60,000 psi. Find life to first crack when loaded as follows: 50,000, 40,000, 30,000 and 20,000 psi. From Figure 12, we find the strain range to be 0.0157 for 1250 cycles which when prorated for the desired load values yield the following predictions:

Load-- $R = 0$ (P/A stress)	Prorated Strain Range	Predicted Life (cycles)	Average Test Life (cycles)
60,000	0.0157 (from Fig.12)	1250 (given)	1250
50,000	0.0131	2700	2700
40,000	0.0104	6500	6500
30,000	0.0078	17,000	17,000
20,000	0.0052	110,000	160,000

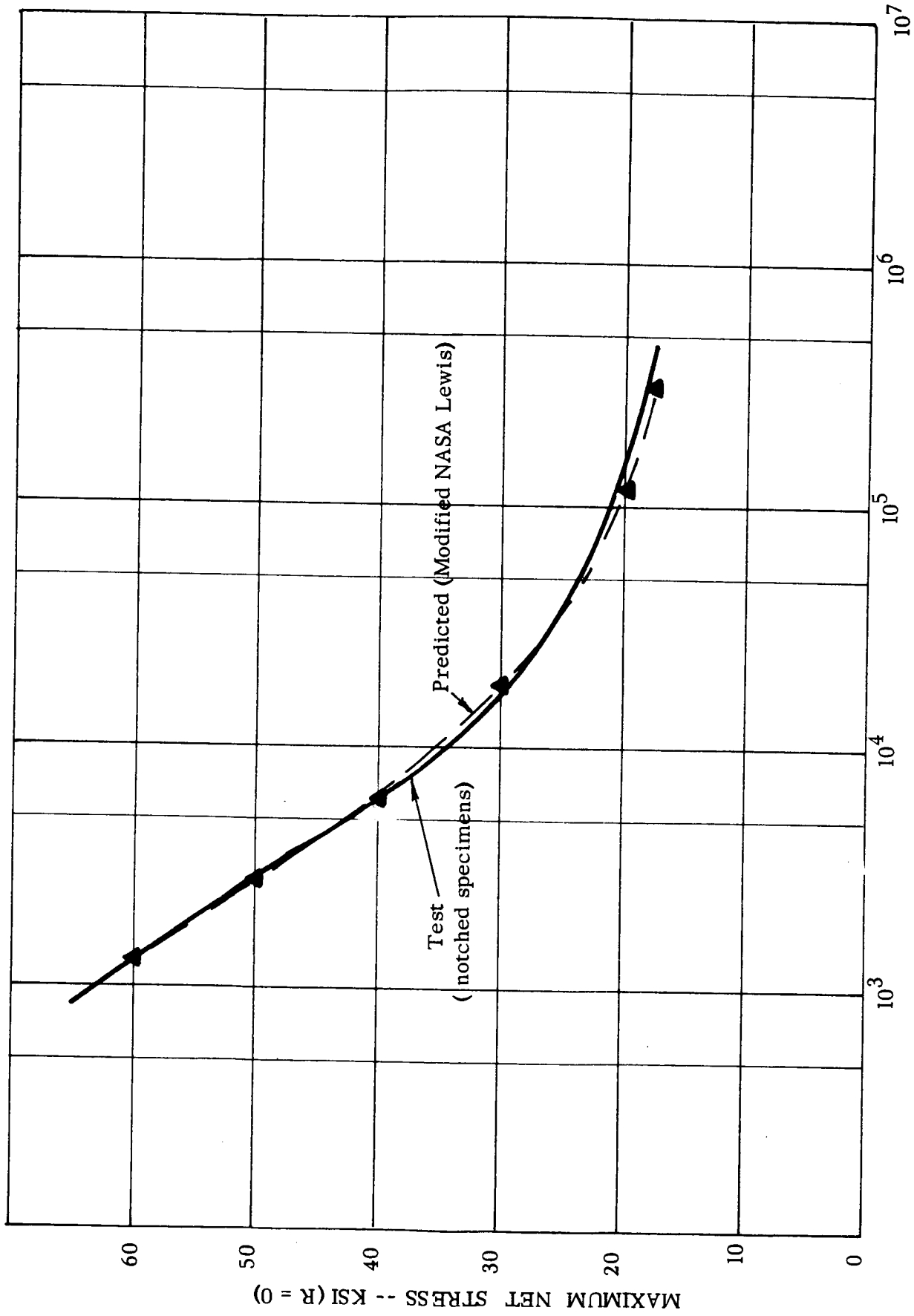
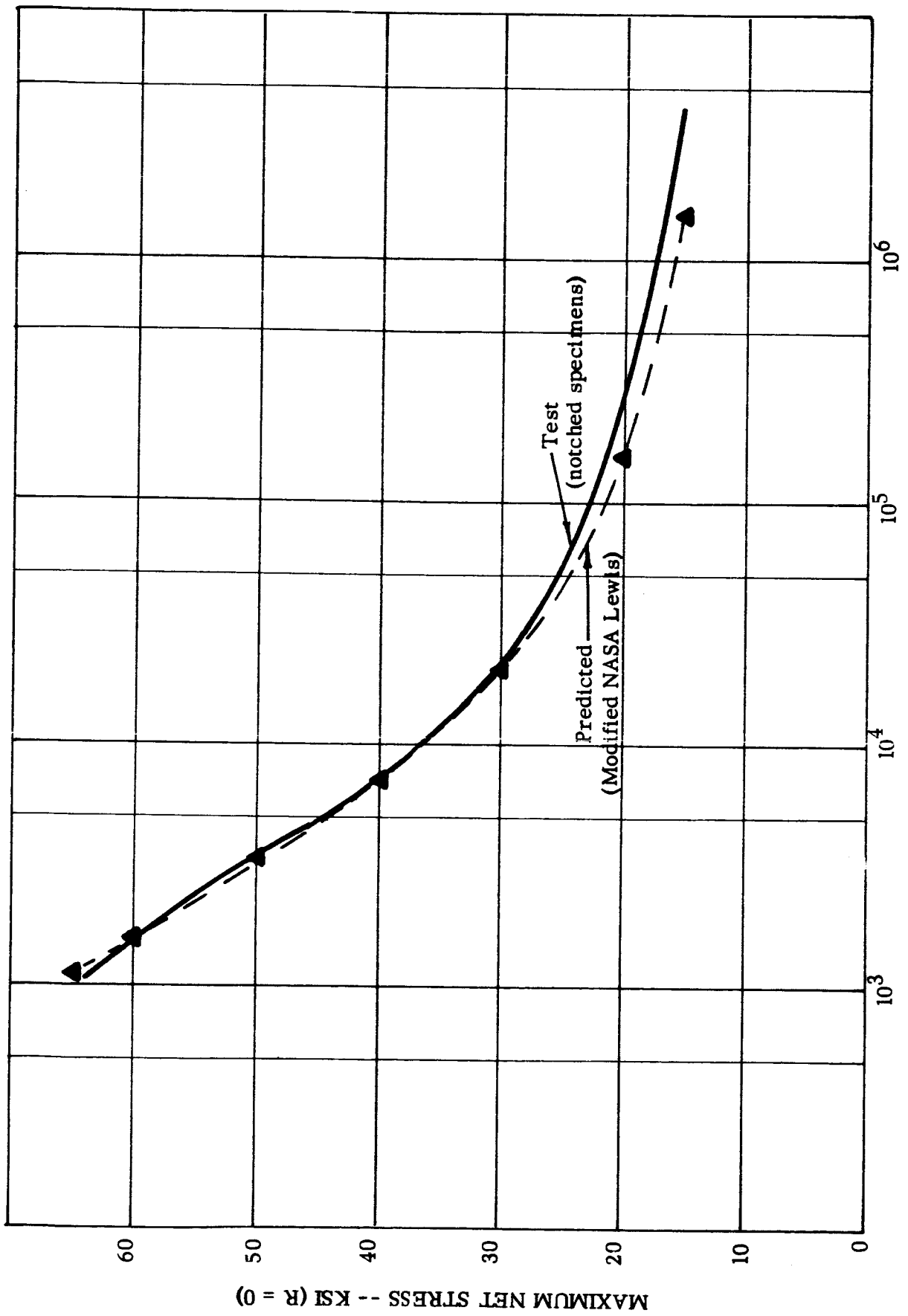


Figure 14. Comparison of Test and Predicted Fatigue Lives to First Crack by Modified NASA Lewis Method



FATIGUE LIFE -- CYCLES

Figure 15. Comparison of Test and Predicted Fatigue Lives to Failure by Modified NASA Lewis Method

4 DISCUSSION

The object of using referenced test datum points for fatigue life prediction is to establish either a stress range or strain range from which remaining S-N or strain-N values can be predicted. By combining the NASA Lewis and Smith methods, an ultimate objective is to predict fatigue life of a part, given only static tensile properties of the material and a single datum point representing the life of the part in the short life ranges. This would eliminate the need for stress concentration, nominal stress, and experimental S-N curves for the material or part.

While good agreement between predictions and test life was had by using either the Smith method or the Modified NASA Lewis method for loading at $R = 0$, there was a decided lack of agreement for cycling at $R = -1$ (Ref. Fig. 10). While test data appear somewhat high in the long life region, this is not an explanation for predictions being very dependent on choice of original test datum points. By contrast, variations in predictions with assumed datum points were surprisingly small for cycling at $R = 0$ as shown in Figures 8 and 9 (Smith method) and in 14 and 15 (Modified NASA Lewis method).

The above indicates a fundamental difference between cycling at $R = 0$ and $R = -1$ where plastic deformation is experienced. When cycling at $R = 0$, the strain at the concentration behaves elastically after a few cycles. Presumably, this is why loads can be prorated directly, using either stress range or strain range. In the case of cycling at $R = -1$, plastic deformation is experienced at each load reversal so that the strain cycling at the concentration is no longer directly proportional to load. A better agreement was had using a variable strain concentration factor (Ref. 6) as shown in Figure 10; however, this presumes a knowledge of nominal stresses and concentration factors which defeats one of the purposes of this investigation.

5 CONCLUSIONS

A method for predicting S-N characteristics of notched specimens (also applicable to fabricated parts) was obtained for 7075-T6 aluminum alloy. Needed information are a single datum point representing short life fatigue strength of the specimen or part, and mechanical properties of the material involved. Neither nominal stresses nor stress concentration are required. Applicability to other materials is a subject for further investigation.

6 REFERENCES

1. Manson, S.S., and Hirschberg, M.H., "Fatigue Behavior in Strain Cycling in the Low and Intermediate Cycle Range", 10th Sagamore Army Materials Research Conf., August 13-16 1963, Sagamore, N.Y.
2. Manson, S.S., "Fatigue: A Complex Subject--Some Simple Approximations", *Experimental Mechanics*, July 1965
3. Smith, Clarence R., "Linear Strain Theory and the Smith Method for Predicting Life of Metals and Structures for Spectrum Loading," Aerospace Research Laboratories Report ARL 64-55, April 1964, Office of Aerospace Research, United States Air Force, Wright-Patterson Air Force Base, Ohio
4. Smith, Clarence R., "A Method for Estimating the Fatigue Life of 7075-T6 Aluminum Alloy Aircraft Structures," Naval Air Engineering Report No. 1096, April 1965
5. Peterson, R.E., Stress Concentration Design Factors, John Wiley & Sons, Inc., New York, 1953
6. Stowell, E. Z., "Stress & Strain Concentration at a Circular Hole in an Infinite Plate," NACA TN 2073, 1950

TABLE I

Mechanical Properties of 0.050-inch Thick 7075-T6 Aluminum Alloy				
Specimen No.	0.2% Offset (PSI)	Ultimate Strength (PSI)	Elongation (Percent)	Percent Reduction in Area
1a	76,300	84,500	11.5	27.3
1b	74,600	82,900	11.5	25.4
2a	79,600	86,700	11.0	27.5
2b	76,300	83,800	10.5	26.8
3a	75,000	84,200	11.0	27.8
3b	77,400	84,000	10.5	31.2
4a	75,500	84,000	12.0	20.8
4b	75,100	83,100	11.5	24.6
5a	77,200	84,200	12.0	26.1
5b	76,300	84,000	10.0	31.0
6a	77,000	84,200	11.0	28.2
6b	77,000	84,000	10.5	25.1
7a	74,500	83,600	11.5	26.5
7b	74,900	83,300	10.5	17.9
8a	76,700	83,900	11.5	25.7
8b	75,300	83,600	11.0	30.8
Average	76,000	84,000	11.1	26.4

TABLE II

Constant-Amplitude Data for Unnotched 0.050-inch 7075-T6 - R = 0

Maximum Stress KSI	Cycles to Failure	Maximum Stress KSI	Cycles to Failure
85.0	3,360	45.0	39,000
85.0	3,490		57,000
			57,000
80.0	2,985		59,000
80.0	4,520		70,000
80.0	6,840		76,000
			134,000
75.0	4,510		152,000
75.0	6,330		259,000
75.0	8,650		291,000
			625,000
65.0	18,000		929,000
65.0	20,000		1,367,000
65.0	22,000		1,383,000
65.0	18,640		
		42.5	76,000
60.0	19,000		
60.0	28,530	40.0	93,000
60.0	29,930	40.0	620,000
60.0	30,290	40.0	10,000,000+
		40.0	12,141,000+
		40.0	12,941,000+
55.0	33,000		
55.0	33,500		
55.0	35,000	35.0	10,183,000+
50.0	41,000		
55.0	52,000		
55.0	59,000		
55.0	65,000		
55.0	76,000		
47.0	59,000		
47.0	147,000		
47.0	298,000		

+ Specimen did not fail

TABLE II, Contd

Constant-Amplitude Data for Unnotched 0.05-inch 7075-T6--R = -0.5 and R = -1

Maximum Stress KSI	Cycles to Failure (R = -0.5)	R = -1			
		Maximum Stress	Cycles to Failure	Maximum Stress	Cycles to Failure
80.0	700	80.0	20	35.0	61,240
80.0	1,080	80.0	24	35.0	73,570
80.0	1,090	80.0	50	35.0	81,000
80.0	1,550	80.0	60	35.0	81,000
				35.0	86,850
75.0	2,670	75.0	203	35.0	89,520
75.0	2,710	75.0	256	35.0	103,000
		75.0	488		
65.0	5,000			27.5	468,000
65.0	6,000	65.0	1,010	27.5	576,000
65.0	9,000	65.0	2,000	27.5	702,000
65.0	11,000	65.0	2,000		
		65.0	2,880	25.0	2,164,000
55.0	16,000	65.0	2,990	25.0	5,829,000
55.0	17,480	65.0	5,000		
55.0	20,000			24.0	2,834,000
55.0	21,000	55.0	8,000		
55.0	23,000	55.0	12,000	23.0	15,439,000+
		55.0	14,000		
45.0	40,000				
45.0	41,000	47.5	24,000		
45.0	45,000	47.5	24,000		
45.0	47,000	47.5	25,000		
35.0	105,000	45.0	20,000		
35.0	272,000	45.0	22,000		
35.0	311,000	45.0	36,000		
35.0	373,000	45.0	37,000		
35.0	1,636,000	45.0	43,000		
31.0	685,000	42.5	35,000		
		42.5	39,000		
30.0	6,289,000	42.5	43,000		
30.0	15,883,000+	42.5	43,000		
30.0	18,117,000				
		40.0	30,910		
		40.0	32,390		
		40.0	35,990		
		40.0	42,990		

+ Specimen did not fail

TABLE III

Constant-Amplitude Data for Notched ($K_t = 2.6$) 7075-T6 --R = -0

Maximum Net Stress KSI	Cycles to		$\frac{\text{Cycles to First Crack}}{\text{Cycles to Failure}}$
	First Crack	Failure	
65.0	790	850	0.929
65.0	880	910	0.967
65.0	945	982	0.962
60.0	1,190	1,240	0.960
60.0	1,190	1,240	0.960
60.0	1,330	1,530	0.869
60.0	1,460	1,560	0.936
55.0	1,680	2,000	0.840
55.0	1,800	2,140	0.841
55.0	1,910	2,160	0.884
55.0	2,140	2,330	0.918
47.5	3,270	3,370	0.970
47.5	3,270	4,140	0.790
47.5	4,500	4,780	0.941
47.5	5,560	6,190	0.898
40.0	3,450	4,870	0.708
40.0	6,000	6,720	0.883
40.0	6,280	7,310	0.859
40.0	7,050	7,960	0.886
40.0	7,120	8,640	0.824
30.0	12,400	14,780	0.840
30.0	11,200	16,630	0.673
30.0	14,950	20,235	0.739
30.0	19,350	23,560	0.821
30.0	22,520	26,490	0.850
20.0	---	54,070	
20.0	47,400	66,270	0.715
20.0	56,000	65,000	0.862
20.0	109,700	118,340	0.927
20.0	114,550	126,120	0.908
20.0	746,000	784,900	0.950
20.0	---	1,251,000	
20.0	----	1,373,500	
20.0	1,782,000	1,785,000	0.998
17.5	466,450	477,340	0.977
17.5	----	205,050	
15.0	----	4,446,000	

TABLE III, Contd

Constant-Amplitude Data for Notched ($K_t = 2.6$) 7075-T6 --R = -0.5 & -0.75			
Maximum Net Stress KSI	Cycles to First Crack	Cycles to Failure R = -0.5	$\frac{N_c}{N_f}$
73.3	70	73	0.959
73.3	65	81	0.802
73.3	---	84	
73.3	65	85	0.765
66.6	---	135	
66.6	125	142	0.880
66.6	150	152	0.987
60.0	210	232	0.905
60.0	210	236	0.890
60.0	210	261	0.805
60.0	---	276	
50.0	---	510	
50.0	600	675	0.889
50.0	600	785	0.764
50.0	750	835	0.898
R = -0.75			
62.8	75	82	0.915
62.8	75	83	0.904
62.8	80	87	0.920
62.8	75	90	0.833
62.8	---	98	

TABLE III, Contd

Constant-Amplitude Data for Notched ($K_t = 2.6$) 7075-T6 -- R = -1									
Maximum Net Stress KSI	Cycles to First Crack (N_c)	Cycles to Failure (N_f)	$\frac{N_c}{N_f}$	Maximum Net Stress KSI	Cycles to First Crack (N_c)	Cycles to Failure (N_f)	$\frac{N_c}{N_f}$		
55.0	---	71		35.0	970	1,490	0.651		
55.0	100	102	0.980	35.0	980	1,570	0.624		
55.0	90	106	0.849	35.0	1,200	1,755	0.684		
55.0	---	110		35.0	1,120	1,810	0.619		
50.0	---	150		35.0	1,350	2,000	0.675		
50.0	---	169							
50.0	98	160	0.613	30.0	4,000	5,000	0.800		
50.0	102	171	0.596	30.0	4,000	5,000	0.800		
50.0	175	200	0.875	30.0	3,700	5,390	0.686		
50.0	---	200		30.0	3,820	5,460	0.700		
50.0	190	210	0.905						
50.0	---	270		25.0	-----	13,700			
				25.0	-----	14,365			
45.0	225	310	0.726	25.0	11,100	16,465	0.674		
45.0	300	350	0.857	25.0	15,000	19,000	0.789		
45.0	270	370	0.730	25.0	18,000	21,000	0.857		
45.0	260	440	0.591	25.0	19,500	21,710	0.898		
45.0	---	475							
40.0	550	640	0.859	20.0	-----	126,000			
40.0	560	650	0.862	20.0	109,000	142,000	0.768		
40.0	555	745	0.745	15.0	114,000	124,000	0.919		
40.0	600	775	0.774	15.0	142,000	151,000	0.940		
40.0	600	825	0.727	15.0	707,000	738,000	0.958		
				15.0	642,000	772,000	0.832		
				15.0	1,607,000	1,640,000	0.979		
				15.0	2,141,000	2,145,000	0.998		
				15.0	2,411,000	2,429,000	0.993		

TABLE III, Contd

Constant-Amplitude Data for Notched ($K_t = 2.6$) 7075-T6 --R = -0.5 & -0.75			
Maximum Net Stress KSI	Cycles to First Crack	Cycles to Failure	$\frac{N_c}{N_f}$
R = -0.5			
73.3	70	73	0.959
73.3	65	81	0.802
73.3	---	84	
73.3	65	85	0.765
66.6	---	135	
66.6	125	142	0.880
66.6	150	152	0.987
60.0	210	232	0.905
60.0	210	236	0.890
60.0	210	261	0.805
60.0	---	276	
50.0	---	510	
50.0	600	675	0.889
50.0	600	785	0.764
50.0	750	835	0.898
R = -0.75			
62.8	75	82	0.915
62.8	75	83	0.904
62.8	80	87	0.920
62.8	75	90	0.833
62.8	---	98	

TABLE III, Contd

Constant-Amplitude Data for Notched ($K_t = 2.6$) 7075-T6 -- R = -1							
Maximum Net Stress KSI	Cycles to First Crack (N_c)	Cycles to Failure (N_f)	$\frac{N_c}{N_f}$	Maximum Net Stress KSI	Cycles to First Crack (N_c)	Cycles to Failure (N_f)	$\frac{N_c}{N_f}$
55.0	---	71		35.0	970	1,490	0.651
55.0	100	102	0.980	35.0	980	1,570	0.624
55.0	90	106	0.849	35.0	1,200	1,755	0.684
55.0	---	110		35.0	1,120	1,810	0.619
50.0	---	150		35.0	1,350	2,000	0.675
50.0	---	169					
50.0	98	160	0.613	30.0	4,000	5,000	0.800
50.0	102	171	0.596	30.0	4,000	5,000	0.800
50.0	175	200	0.875	30.0	3,700	5,390	0.686
50.0	---	200		30.0	3,820	5,460	0.700
50.0	190	210	0.905				
50.0	---	270		25.0	-----	13,700	
				25.0	-----	14,365	
45.0	225	310	0.726	25.0	11,100	16,465	0.674
45.0	300	350	0.857	25.0	15,000	19,000	0.789
45.0	270	370	0.730	25.0	18,000	21,000	0.857
45.0	260	440	0.591	25.0	19,500	21,710	0.898
45.0	---	475					
40.0	550	640	0.859	20.0	-----	126,000	
40.0	560	650	0.862	20.0	109,000	142,000	0.768
40.0	555	745	0.745	15.0	114,000	124,000	0.919
40.0	600	775	0.774	15.0	142,000	151,000	0.940
40.0	600	825	0.727	15.0	707,000	738,000	0.958
				15.0	642,000	772,000	0.832
				15.0	1,607,000	1,640,000	0.979
				15.0	2,141,000	2,145,000	0.998
				15.0	2,411,000	2,429,000	0.993

**REPORT DISTRIBUTION LIST FOR
CONTRACT NAS3-7268**

- | | |
|---|--|
| <p>1. NASA Scientific and Technical Information Facility (6)
Box 5700
Bethesda, Maryland
Attention: NASA Representative</p> | <p>9. NASA Lewis Research Center (1)
21000 Brookpark Road
Cleveland, Ohio 44135
Attention: Dr. W.W. Roudebush M.S. 60-6
Air-Breathing Engine Division</p> |
| <p>2. NASA Headquarters (1)
FOB-10B
600 Independence Ave., S.W.
Washington, D.C. 20546
Attention: N.F. Rekos (RAP)</p> | <p>10. NASA Lewis Research Center (1)
21000 Brookpark Road
Cleveland, Ohio 44135
Attention: Albert E. Anglin M.S. 60-6
Air-Breathing Engine Division</p> |
| <p>3. NASA Lewis Research Center (1)
21000 Brookpark Road
Cleveland, Ohio 44135
Attention: Report Control Office M.S. 5-5</p> | <p>11. NASA Lewis Research Center (3)
21000 Brookpark Road
Cleveland, Ohio 44135
Attention: Marvin Hirschberg M.S. 49-1</p> |
| <p>4. NASA Lewis Research Center (1)
21000 Brookpark Road
Cleveland, Ohio 44135
Attention: Library MS. 60-3</p> | <p>12. NASA Lewis Research Center (1)
21000 Brookpark Road
Cleveland, Ohio 44135
Attention: John DeFord M.S. 60-5
Air-Breathing Engine Procurement</p> |
| <p>5. NASA Lewis Research Center (1)
21000 Brookpark Road
Cleveland, Ohio 44135
Attention: Technology Utilization
Office M.S. 3-19</p> | <p>13. FAA Headquarters
800 Independence Ave., S.W.
Washington, D.C. 20553
Attention: Gordon M. Bain SS/120 (1)
Jack O. Charshafian (1)</p> |
| <p>6. NASA Lewis Research Center (1)
21000 Brookpark Road
Cleveland, Ohio 44135
Attention: I.I. Pinkel M.S. 5-3
Fluid System Components Div.</p> | <p>14. Supersonic Transport Office
Wright-Patterson AFB, Ohio 45433 (1)
Attention: SESHS, J.L. Wilkins</p> |
| <p>7. NASA Lewis Research Center (1)
21000 Brookpark Road
Cleveland, Ohio 44135
Attention: Thomas B. Shillito M.S. 5-3
Fluid System Components Division</p> | <p>15. Aeronautical Systems Division
Wright-Patterson AFB, Ohio
Attention: ASRTCE/Harold K. Triulio (1)
AFAPL(APIE)/Robert Supp (1)
Directorate of Materials &
Processes</p> |
| <p>8. NASA Lewis Research Center (1)
21000 Brookpark Road
Cleveland, Ohio 44135
Attention: J. Howard Childs M.S. 60-4
Air-Breathing Engine Division</p> | <p>16. Air Force Office of Scientific Research
Propulsion Research Division
USAF Washington 25, D.C.
Attention: Dr. M. Slawsky (1)</p> |

16. AFWL (1)
Kirtland Air Force Base, New Mexico
Attention: WLPC/ Capt. C.F. Ellis
18. Defense Documentation Center (DDC) (1)
Cameron Statich
5010 Duke Street
Alexandria, Virginia 22314
19. AFML (MAMP)
Wright-Patterson AFB, Ohio 45433
Attention: Mr. S. Inouye
(1) AFML (MATP)
Attention: Mr. G.A. Gegel (1)
(2) AFML(MAAM) Library (1)
Wright-Patterson AFB, Ohio, 45433
20. Department of the Navy (1)
ONR
Code 429
Washington 25, D.C.
Attention: Dr. R. Roberts
21. Chief, Bureau of Naval Weapons (1)
Dept. of the Navy
Washington 25, D.C.
Attention: RRMA-2
22. NASA-Langley Research Center (1)
Technical Library
Langley Field, Virginia
23. Jet Propulsion Laboratory (1)
4800 Oak Grove Drive
Pasadena, California 91102
Attention: R.W. Hardt
24. General Dynamics/Convair (1)
Interplant Zone 578-20
P.O. Box 1950
San Diego California
Attention: C.R. Smith
25. University of Illinois
Dept. of T. & A M
Urbana, Illinois
Attention: Prof. T. Dolan (1)
Prof. JoDean Morrow (1)
26. Michigan Technological University (1)
Dept. of Engineering Mech.
Houghton, Michigan
Attention: Prof. C.E. Work
27. Pennsylvania State University (1)
Dept. of Eng. Mechanics
University Park, Pennsylvania
28. Technion Research & Development
Foundation Ltd. (1)
Technion Israel Inst. Of Tech.
Haifa, Israel
Attention: A. Berkovitz
29. Syracuse University
Dept. of Chemical Eng. and Metallurgy
Syracuse, New York 13210
Attention: Dr. V. Weiss (1)
Dr. H.W. Liu (1)
30. Columbia University (1)
632 West 125th Street
New York 27, New York
Attention: Prof. A.M. Freudenthal
31. NASA-Langley Research Center (1)
SRD-Fatigue Branch
Langley Field, Virginia
Attention: Mr. H.F. Hardrath
32. Brown University (1)
Division of Engineering
Providence, R.I.
Attention: Prof. W.N. Findley
33. Mr. J.J. O'Brien (1)
Consulting Engineer
1119 28th Street
San Diego, California
34. TRW Inc. (1)
TRW Materials & Processing Dept.
23555 Euclid Avenue
Cleveland, Ohio 44117
Attention: Dr. A. Nemy